



Designing, cloning and simulation studies of cancer/testis antigens based multi-epitope vaccine candidates against cutaneous melanoma: An immunoinformatics approach

Sana Khalid ^a, Jinlei Guo ^b, Syed Aun Muhammad ^{a,*}, Baogang Bai ^{c,d,e,**,1}

^a Institute of Molecular Biology and Biotechnology, Bahauddin Zakariya University Multan, Pakistan

^b School of Intelligent Medical Engineering, Sanquan College of Xinxiang Medical University, Xinxiang, China

^c School of Information and Technology, Wenzhou Business College, Wenzhou, China

^d Zhejiang Province Engineering Research Center of Intelligent Medicine, Wenzhou, China

^e The 1st School of Medical, School of Information and Engineering, The 1st Affiliated Hospital of Wenzhou Medical University, Wenzhou, China

ARTICLE INFO

Keywords:

Cutaneous melanoma
Tumor associated antigens
Chimera vaccine
Machine learning
Vaccinomics

ABSTRACT

Background: Melanoma is the most fatal kind of skin cancer. Among its various types, cutaneous melanoma is the most prevalent one. Melanoma cells are thought to be highly immunogenic due to the presence of distinct tumor-associated antigens (TAAs), which includes carcinoembryonic antigen (CEA), cancer/testis antigens (CTAs) and neo-antigens. The CTA family is a group of antigens that are only expressed in malignancies and testicular germ cells.

Methods: We used integrative framework and systems-level analysis to predict potential vaccine candidates for cutaneous melanoma involving epitopes prediction, molecular modeling and molecular docking to cross-validate the binding affinity and interaction between potential vaccine agents and major histocompatibility molecules (MHCs) followed by molecular dynamics simulation, immune simulation and *in silico* cloning.

Results: In this study, three cancer/testis antigens were targeted for immunotherapy of cutaneous melanoma. Among many CTAs that were studied for their expression in primary and malignant melanoma, NY-ESO-1, MAGE1 and SSX2 antigens are most prevalent in cutaneous melanoma. Cytotoxic and Helper epitopes were predicted, and the finest epitopes were shortlisted based on binding score. The vaccine construct was composed of the four epitope-rich domains of antigenic proteins, an appropriate adjuvant, His tag and linkers. This potential multi-epitope vaccine was further evaluated in terms of antigenicity, allergenicity, toxicity and other physicochemical properties. Molecular interaction estimated through protein-protein docking unveiled good interactions characterized by favorable binding energies. Molecular dynamics simulation ensured the stability of docked complex and the predicted immune response through immune simulation revealed elevated levels of antibodies titer, cytokines, interleukins and immune cells (NK, DC and MA) population.

Conclusion: The findings indicate that the potential vaccine candidates could be effective immunotherapeutic agents that modify the treatment strategies of cutaneous melanoma.

1. Introduction

Melanoma is the malignancy of melanocytes [1]. In the last few decades, occurrence of melanoma has expanded in developed, particularly fair-skinned nations and now melanoma is the fifth most common cancer in the United States [2]. Unlike the majority of cancers, the

incidence of melanoma is not strongly related to age, and is most frequent among people aged 20 to 35. Melanoma is a prime example of how genetic and environmental factors affect the cancer pathogenesis. Race and locality have a significant impact on its incidence [3]. Due to the lack of effective systemic medicines, there has been little progress in the therapy of metastatic melanoma [4]. Over the last decade, we've

* Corresponding author.

** Corresponding author. School of Information and Technology, Wenzhou Business College, Wenzhou, China.

E-mail addresses: aunmuhammad78@yahoo.com (S.A. Muhammad), 20190165@wzbc.edu.cn (B. Bai).

¹ These authors contributed equally to this work.

learned a lot more about the immunosuppressive tumor microenvironment. To generate immunogenicity, cancer cells express antigens on their surface which are capable of eliciting immune response [3]. For the successful development of immunotherapy, the determination of pertinent tumor specific antigens is essential. Because of well-known tumor-associated antigens (TAAs) like cancer-testis antigens (CTAs) harboring novel self-antigen epitopes, melanoma cells are regarded as being highly immunogenic. The cancer/testis antigen (CTA) family is exclusively expressed in the germ cells of the testis and in different types of cancer. According to their origin, function, or pattern of expression, they are classified into few classes that are silent in normal cells aside from germ cells but are aberrantly produced in tumor cells [5]. More than 100 CTA gene families have been discovered thus far. The bulk of these genes have a high degree of sequence homology and are found on the X-chromosome. The expression of cancer-testis antigens (CTAs) has been observed for the first time in melanoma. Many CTAs have been observed in melanoma samples, particularly those that have the ability to spread metastatically. Numerous of them have been demonstrated to have oncogenic effects by altering crucial melanoma-related pathways. CTAs are potential targets for immunotherapy due to their critical role in the aetiology and prevalence of cutaneous melanoma. Several clinical trials are currently being conducted to assess the benefits of antigen-based immunotherapeutic on melanoma patients. The antigens MAGE and NY-ESO-1 currently show the most promise affect [6]. MAGE family has received the greatest research attention among any CTA to yet [7,8]. Initially identified from melanoma, the melanoma antigen (MAGE) genes exhibit tumor-specific expression pattern. Thus, MAGE genes were consequently suggested as prospective targets and MAGE peptide vaccine constructs are being tested in clinical trials as potential immunizing agents [9]. Recently, it was discovered that the SSX2 gene was expressed in melanomas when looking for melanoma tumor antigens [10] as well as several more cancers. Additionally, it was shown that a fraction of melanoma patients may respond humorally to the SSX2 protein, which is also known as HOM-MEL-40, as a tumor-associated antigen [11]. A significant portion of individuals with advanced NY-ESO-1-expressing cancer cells experience concurrent cellular mediated and humoral immune responses in response to the highly immunogenic CT antigen NY-ESO-1 [12].

The protracted traditional methods of drug testing and vaccine design demand perseverance, arduous effort, exorbitant expense, and more staff. It has never been simple to test and experimentally validate thousands of compounds for a particular medicinal feature. The delivery of either a whole or attenuated pathogen during a standard immunization poses toxicity and safety concerns. The concept of enhanced vaccination based on epitopes—small peptides that can trigger a particular immune response—was made possible by the development of sequencing and recombinant DNA technologies. With the advent of bioinformatics, creating vaccines and medications has benefited. In the past two decades, a variety of *in silico* technologies have been created to construct immunotherapy and peptide-based medications. These tools proved to be a catalyst in drug and vaccine designing [13]. Cutting-edge software tools and databases have become crucial in the designing of vaccines. Advanced epitope prediction software, such as NetMHC and BepiPred [14], facilitates the identification of T-cell and B-cell epitopes within target antigens. Furthermore, structural analysis tools like PyMOL [15] and UCSF Chimera [16], along with AI-driven approaches like AlphaFold [17], contribute to the accurate modeling of protein structures, enabling a comprehensive understanding of the spatial arrangement and interactions of epitopes. Immunoinformatics tools, including C-Immsim [18] and NetVac [19], predict immunogenicity, while databases like the Immune Epitope Database (IEDB) offer curated epitope information. Overall, these state-of-the-art technologies collectively empower researchers in the strategic and efficient design of multi-epitope vaccines, advancing the frontier of vaccine development.

This study attempted to design a suitable, universally applicable multi-epitope chimera vaccine candidate against cutaneous melanoma

by targeting the melanoma-specific antigenic proteins. Epitopes were predicted through the utilization of multiple well-established databases (NetMHCpan-4.1a, IEDB, BepiPred 2.0) to facilitate cross-validation, and subsequently, overlapping epitopes were chosen for further consideration. Epitope-rich domains of selected CTAs were linked together with linkers along with suitable molecular adjuvant. The secondary structure prediction relied on PSIPRED 4.0 [19] and GOR [20], while the tertiary structure prediction was done through an AI program AlphaFold developed by DeepMind. Protein-protein docking analysis by ClusPro server [15] elucidated the molecular interactions between our vaccine construct and immune system receptors. Molecular Dynamic Simulation conducted through GROMACS software [21] and Immune simulation via C-Immsim elucidated the stability and theoretical immune response of our vaccine candidate. We believed that our vaccine construct can be a valuable therapy for cutaneous melanoma, however immune response, efficacy and safety could be experimentally verified.

2. Materials and methods

2.1. Selection of tumor-associated CTAs

Three melanoma-specific Cancer/Testis antigens were selected i.e., NY-ESO-1 (Gene: CTAG1A; CTAG1B), Melanoma-associated antigen E1 (Gene: MAGEE1) and Protein SSX2 (Gene: SSX2; SSX2B). These antigens were selected based on their prevalence and high expression in primary and malignant cutaneous melanoma [22]. Antigenicity of selected proteins was predicted by VaxiJen (<http://www.ddg-pharmfac.net/vaxijen/VaxiJen/VaxiJen.html>). VaxiJen is the firstly developed online tool to predict probable antigens of bacteria, viruses and tumors [23]. ToxinPred was used to predict toxicity (<http://crdd.osdd.net/raghava/toxinpred/>). [24]. ProtParam was used to predict Molecular weight, instability index, pI and half-life. (www.expasy.org/protparam/). ProtParam predicts proteins physicochemical properties. SOLPro was used to check protein's solubility (<https://scratch.proteomics.ics.uci.edu/>) offered by Scratch Protein Predictor [25]. Prot p (www.protpi.ch/Calculator/ProteinTool) was used for the calculation of net charge.

2.2. Sequence retrieval

To start with, amino acid sequences of our selected oncofetal proteins NY-ESO-1 (CAA05908), MAGE-1 (NP_004979) and SSX2 (CAA60111) was fetched in FASTA format from NCBI database and were subjected to further examination (www.ncbi.nlm.nih.gov/).

2.3. Cytotoxic T-cells (MHC-I) epitopes prediction

Cytotoxic T-cells recognizes antigen bound with MHC-I molecules. Binding with CTLs was predicted by NetMHCpan-4.1a (www.services.healthtech.dtu.dk/services/NetMHCpan-4.1a/) and also from IEDB (<http://tools.iedb.org/main/tcell/>). NetMHCpan predict pan specific binding of any peptide with known sequences [26]. Epitopes were predicted using seven HLA alleles covering majority of human population. Threshold for strong and weak binders were 0.5 % and 1 % respectively. All strong binder epitopes of 9AA with high CTL scores were selected.

2.4. Helper T-cells (MHC-II) epitopes prediction

MHC-II class molecules activates Helper T-lymphocytes which in turn release cytokines that elicit other immune responses. Binding of our selected protein with HTLs was predicted by NetMHCIIpan-4.0 (www.services.healthtech.dtu.dk/services/NetMHCIIpan-4.0/) and IEDB (<http://tools.iedb.org/main/tcell/>) [27]. Common HLA alleles were considered. All strong binders with were selected. This server uses artificial neural network (ANN). All predicted binders of 9AA having high score and with threshold 1 % were selected. High score indicated high affinity.

2.5. Prediction of B-cell epitopes

BepiPred 2.0 and Kolaskar and Tongaonkar antigenicity methods by IEDB (<http://tools.iedb.org/bcell/>) predicted peptide interaction with B-cell to trigger a humoral immune response at 0.5 and 1.0, respectively. BepiPred 2.0 sequentially predict antigenic determinants of amino acids and Kolaskar and Tongaonkar Antigenicity predict B-cell epitopes on the basis of their physicochemical properties and their occurrence in recognized epitopes [28].

2.6. Construction of final multi-epitope vaccine

Those peptide domains that were covering most of the MHC-I, MHC-II, HTCs, CTCs and B-cell epitopes were selected manually and joined with AAY(Alanine-Alanine-Tyrosine) linker. An adjuvant 50S ribosomal protein L7/L12 (P9WHE3.1) was added at the 'N' terminus of fusion protein by EAAAK linker. RVR linker was used to attach a 6xHis tag to the 'C' terminus for easy identification. To avoid any autoimmune response, screening by BLASTp was done against the Uniprot database (www.uniprot.org/blast) to check homology of our vaccine construct with human proteome. Antigenicity of each subunit was predicted form VaxiJen (www.ddg-pharmfac.net/vaxijen/VaxiJen/VaxiJen.html).

2.7. Antigenicity, allergenicity and other physicochemical analysis

Size, theoretical Pi, molecular weight, GRAVY (measure of hydrophobicity) and instability index were predicted from ProtParam by ExPaSy (<https://web.expasy.org/protparam/>). The ProtParam tool computes protein's physicochemical properties. For idealized multi-epitope vaccine candidates, size should be less than 100 kb [29], theoretical Pi should be around 7 [30], molecular weight should be 30–100 kDa, a balanced GRAVY score should be close to zero [31]. All these values were kept in consideration during the screening process. ProtParam results classified this fusion protein as stable protein. Antigenicity was predicted from VaxiJen (<http://www.ddg-pharmfac.net/vaxijen/VaxiJen/VaxiJen.html>) and AntigenPro offered by Scratch Protein Predictor (<https://scratch.proteomics.ics.uci.edu/>). AntigenPro predict antigenicity based on data from protein microarrays rather than conventional homology based prediction [32]. ToxinPred predicted toxicity (<http://crdd.osdd.net/raghava/toxinpred/>), and AllerTOP server 2.0 predicted allergenicity (www.ddg-pharmfac.net/AllerTOP/). AllerTOP predict allergens and route of allergens with the sensitivity of almost 94 % [33]. SOLPro was used form the predicted of solubility (www.scratch.proteomics.ics.uci.edu/). The solubility of proteins based on SVM method was predicted by SOLPro with the estimated accuracy of 74 % [34].

2.8. Human population coverage analysis

Population coverage of our vaccine candidate was analyzed against seven most common alleles of HLA class I and seven alleles of HLA class II by IEDB (<http://tools.iedb.org/population/>). The population coverage analysis was done worldwide.

2.9. Prediction of secondary structure

PSIPRED 4.0 server predicted secondary structure(<http://bioinf.cs.ucl.ac.uk/psipred/>) and GOR (https://npsa-prabi.ibcp.fr/cgi-bin/scpred_gor4.pl) PSIPRED is a reliable approach to predict the secondary structure of proteins using PSI-BLAST. (Position Specific Altered BLAST) [35].

2.10. Prediction and refinement of tertiary structure

Tertiary structure of vaccine construct was predicted from Alphafold incorporated into ChimeraX (<https://www.rbvi.ucsf.edu/chimerax/>). Alphafold is an Artificial Intelligence based Program developed by

DeepMind that quite accurately predict the 3 dimensional structure of protein [36]. GalaxyRefine enhanced this Alphafold predicted structure (<https://galaxy.seoklab.org/cgi-bin/submit.cgi?type=REFINE>). Among 5 models refined by GalaxyRefine, best quality model (MODEL 1) was selected based on Molprobity, class score, GDT-HA score and RMSD score.

2.11. Validation of tertiary structure

For the validation of refined vaccine structure, ProSA web server (<https://prosa.services.came.sbg.ac.at/prosa.php>) was used for the evaluation of overall model quality and Z-score. ProSA server (Protein Structural Analysis) predict the errors in experimental structural models of protein [37]. Ramachandran plot analysis and other features were examined by MolProbity (<http://molprobity.biochem.duke.edu/>). Hydrogen atoms were added and all-atoms contacts and geometry were analyzed without the prediction of flip-errors. MolProbity server allows the broad-spectrum validation and evaluation of model structural quality. It relies on the optimized hydrogen placement and covalent-geometry and angle criteria [38].

2.12. Prediction of conformational epitopes

ElliPro server predicted new conformational epitopes from a 3d improved model (<http://tools.iedb.org/elliopro/>). 6 epitopes were selected having score ranging from 0.8-0.7. ElliPro server relies on the geometrical features of protein and allow the prediction of epitopes either from protein sequence or structure [39]. The overlapping B and T cell epitopes were then modeled on the surface chimera protein using the ChimeraX software.

2.13. Molecular docking

Structures of human TLR4 (PDB ID: 4G8A) and HLA-A*11:01 with GTS1 peptide (PDB ID: 5WJL) were downloaded from PDB database [40]. Both these structures and our vaccine construct were prepared for docking by Dockprep in UCSF chimera software. During Dockprep, hydrogen atoms and charges were added. For protein-protein molecular docking, ClusPro server (<https://cluspro.org/home.php>) was used for the molecular docking of our multi-epitope vaccine construct as a receptor with TLR4 and HLA-A*11:01 as a ligand. Among 29 models generated by ClusPro server, models having the lowest energy were selected. ClusPro server is widely used for molecular docking and provide a number of advanced option for the modification of protein models [41]. Pymol software (<https://pymol.org/2/>) was used to illustrate the docked models. Pymol is a graphic tool for 3d visualization of proteins [42].

2.14. Molecular dynamics simulation

Molecular Dynamic simulations utilized the docked complexes generated by the Cluspro server. Given the protein-protein nature of the complexes, characterized by multiple chains, the MD simulations were computationally executed on the High-Performance Computing (HPC) cluster using the Gromacs 2020.4 MD simulation package [31]. The preparation of protein chain topologies involved the utilization of the CHARMM-36 force field parameters [43]. Each receptor system, in conjunction with the associated bound vaccine, underwent solvation using the single point charge water model within dodecahedron unit cells. The system was further neutralized through the incorporation of Na⁺ or Cl⁻ counter-ions. The solvated systems underwent an initial energy minimization process to alleviate potential steric clashes, utilizing the steepest descent criteria until the threshold (Fmax < 10 kJ/mol) was attained. Following energy minimization, the systems underwent equilibration under constant volume and temperature conditions at 300 K, employing a modified Berendsen thermostat.

Table 1
Amino Acid sequences of selected antigenic proteins retrieved from NCBI.

Protein	Accession Number	UniProt ID	Sequence
Cancer/testis antigen 1 (NY-ESO-1)	CAA05908	P78358 · CTG1B_HUMAN	>CAA05908.1 NY-ESO-1 protein [Homo sapiens] MQAEGRGTTGGTGDADPGPGIPDGGNAGGPGAEAGATGGRGPRGAGAAASASGPGGGAPRGGHGGGAASGLNGCCRCGARGPESRL LEFYLAIPFAIPMEAEELARRSLAQDAPPVPGVLLKEFTVSGNLTIRLTAADHRQLQLSISSCLQQLSILLMWTQCFLPVLVLAQPFGGQRR
Melanoma-associated antigen E1 (MAGE-1)	NP_004979	Q9HC15 · MAGE1_HUMAN	>AAA03229.1 MAGE-1 [Homo sapiens] MSLEFORSLSHGCKPEEALAQOEALGLVQVQAAATSSSSPLVLGTLVEEPTAGSTDPQSPQOGASAFPPTTINFTRORQPSGSSSREEGPSTSCI LESLEFRVITKVAADLVGFLLLKYRAREPVTKAEMLESVKNYKHCFFEIFGKASESLQVFGIDVKEADPTGHSYLVITCLGLSYDGLLGDN QIMPKTGFLIIVLMIAEMEGGHAPPEEWEELSVMVEVDGREHSAYGEPRKLLTQDLVQEKYLEYRQVPDSDPARYEFWGWPRALAEYSY VKVLEYVYKVSARVRFPPFSLREAAALREEEGV
Protein SSX2	CAA60111	Q16385 · SSX2_HUMAN	>CAA60111.1 SSX2 [Homo sapiens] MNGDDAFARRPTVGAQIPEKIQKAFDDIIAKYFSEEWKMKASEKIFVYMKRKYEAMTKLGFKATLPPFMCNKRKRAEDFQGNLDLNDP NRGNQVERPQMTFGRLLQGISPKIMPKPAEEGNDSEEVPEASGPQNDGKELCPGKPTTSEKHERSGPKRGEHAWTHRLRERKQLVI YEEISDPEEDE

Subsequently, an additional equilibration step was conducted under constant volume and pressure, employing the Berendsen barostat, each for a duration of 100 ps. The equilibrated systems were subsequently subjected to a 50 ns production phase of molecular dynamics (MD) simulations. The resultant trajectories were subjected to analysis, including assessments of root mean square deviations (RMSD) in protein backbone atoms, root mean square fluctuations (RMSF) in the side chain atoms of individual chains within each protein complex and the radius of gyration (Rg) [44].

2.15. Codon optimization and cloning

Java Codon Optimization Tool was used to optimize the codons (<http://www.jcat.de/>). JCat is a novel and rapid method that uses the most common sequenced prokaryotic and eukaryotic hosts for recombinant protein expression [45]. Two common restriction sites were added at both ends of codon and was cloned in pET28a(+) vector using Snapgene software available at <https://www.snapgene.com/>.

2.16. Immune simulation

To check the interaction of our vaccine candidate with the components of immune system of humans, computational immune simulation was done. C-ImmSim server was used (<https://kraken.iac.rm.cnr.it/C-IMMSIM/>). Three injections were administered at the time step of 1 and 63 (each time step is about 8h). 1000 antigens were given with no LPS. Simulation steps were set at 1050 while all other parameters were at their default [46].

3. Results

3.1. Sequence retrieval and antigenicity prediction

Our selected tumor antigens i.e., Cancer/testis antigen 1 or NY-ESO-1 (CTAG1A; CTAG1B), Melanoma-associated antigen E1 (MAGE1) and Protein SSX2 (SSX2; SSX2B) have their role in the prognosis of different carcinomas and can be used as a potential aim for immunotherapy of cancer. The FASTA sequences of selected oncofetal proteins were extracted from GenBank database of NCBI (Table 1). These proteins, among the other cancer testis antigens, were shortlisted on the basis of their antigenicity, allergenicity and other physical and chemical properties. Antigenicity of selected proteins predicted by VaxiJen indicated the significant outcomes. VaxiJen uses sequence alignment for the prediction of probable antigens [47]. Toxicity analysis showed that these potential vaccine candidates are non-toxin. Other physical and chemical properties showed the compatible results at standard cut off parameters (Table 2).

3.2. Cytotoxic T-cell epitopes prediction

Cytotoxic T-lymphocytes binds with the MHC class I and contributes to immunogenic administration of the endogenous and exogenous antigens [48]. T cell epitope prediction is considered as the most selected step in vaccine designing. IEDB and NetMHCpan-4.1a server were utilized for predicting cytotoxic T-cell epitopes and all ranked 9AA epitopes were selected with wide spectral alleles of HLA_A0201, HLA_A0204, HLA_A0206, HLA_B0702, HLA_B51, HLA_B5301 and HLA_B5401. Total 84 epitopes of three selected oncofetal proteins were identified by IEDB server (Supplementary Table 1) and 67 epitopes (Supplementary Table 2) were selected from NetMHCpan- 4.1a. Among these, overlapping epitopes were designed as the part of final vaccine construct.

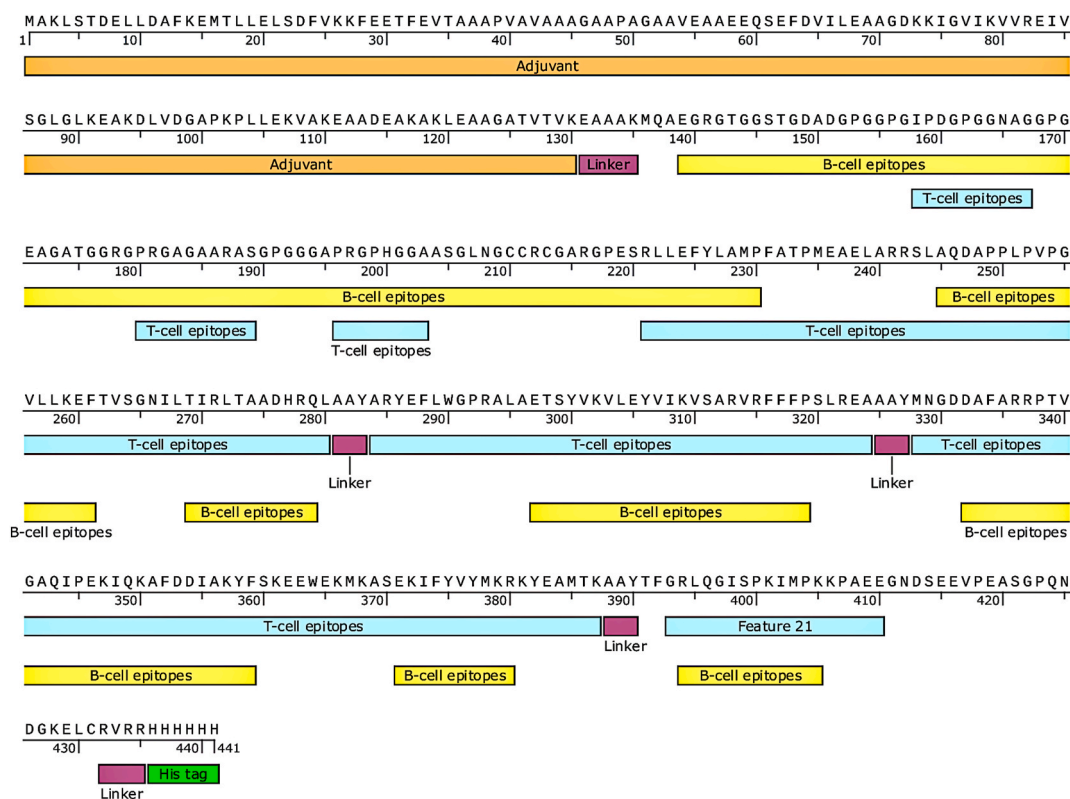
3.3. Helper T-cell epitopes prediction

Helper T lymphocytes recognize complex of foreign antigens bind with MHC-II and release a series of signaling molecules called cytokines

Table 2

Physicochemical properties of ranked antigenic proteins predicted using VaxiJen, ToxinPred, UniProt, ProtParam, Pro pI, and SolPro servers.

Protein	Gene	Size	MW (Da)	Antigenicity	Toxicity	Solubility	pI	Half-life	Instability index	Charge (pH 7.4)
Cancer/testis antigen 1 (NY-ESO-1)	CTAG1A; CTAG1B	180aa	17,992	0.6774	Non-toxin	0.94429	8.79	>30 h	43	1.787
Melanoma-associated antigen E1	MAGEE1	957aa	103,254	0.4032	Non-toxin	0.7737	4.83	>30 years	51.58	-18.128
Protein SSX2	SSX2; SSX2B	188aa	21,620	0.3929	Non-toxin	0.88164	5.59	>30 years	53.7	-4.885

**Fig. 1.** Sequence of 441AA multi-epitope vaccine candidate. Features showing the B and T cell epitopes, adjuvant and 6x his tag. Diagram was created by SnapGene software.

which eventually elicit a series of immune response [49]. We predicted Helper T-cell epitopes by Immune Epitope Database (IEDB) and NetMHCIIpan- 4.0. All 9AA epitopes having high binding score were selected with the most common HLA alleles in the worldwide population i.e., HLA_DRB1*0101, HLA_DRB1*0401, HLADRB1*0402, HLA_DRB1*0701, HLA_DRB1*0801, HLA_DRB1*1101 and HLA_DRB1*1501. Total 67 IEDB predicted epitopes and 58 NetMHCIIpan-4.0 predicted epitopes were considered (Supplementary Tables 3 and 4).

3.4. B-cells epitopes prediction

B-cell induce humoral immunity by producing antibodies and have important role in tumor microenvironment. BepiPred Linear Epitope

Prediction 2.0 and Kolaskar and Tongaonkar Antigenicity methods server was used for the prediction of linear B-cells epitopes. Almost 15 epitopes were shortlisted and are part of the final vaccine construct (Supplementary Table 5).

3.5. Final multi-epitope vaccine construction

Epitope rich domains of three selected antigenic proteins were merged to create a multi-epitope vaccine candidate by AAY linker. A Molecular adjuvant (MAKLSTDELLDAFKEMTLLELSDFVKKFEETFEV TAAAPVAVAAAGAAPAGAAVEAAEQSEFDVILEAAGDKKIGVIVKVVREI VSGLGLKEAKDLVDGAPKPLLEKVAKEAADEAKAKLEAAGATVTVK) was joined to intensify the magnitude of immune response. The final vaccine

Table 3

Four epitope rich domains were selected. These subunits cover most of the T cell and B cell epitopes. Antigenicity of Individual domains was predicted by VaxiJen.

Subunits	Antigen	Position	Sequence	Antigenicity
Subunit A	NY-ESO-1	1–145	MQAEGRGTGGSTGDADGPGGPGIPDGPGGNAGGPGEGAGATGGRGPRGAGAARASGPG GAPRPHGGGAASGLNGCCRCGARGPESRLLLEFYLAMPPFATPMEAE LARRSLAQDAPPLVPPGVLLKEFTVSGNILTIRLTAADHRQL	0.7565
Subunit B	MAGE-1	260–300	ARYEFLWGPRLAETS YVVKVLEYVIKVSARVRRFFPSLREA	0.4484
Subunit C	SSX-2	1–60	MNGDDAFARRPTVGAQIPEKI QKAFDDIAKYFSKEEWEKMKASEKIFVYVMKRKYEAMTK	0.371
Subunit D	SSX-2	100–140	TFGR LQGISP KIMP KPAEEGNDSEEVPEASGPQNDGKELC	0.7706

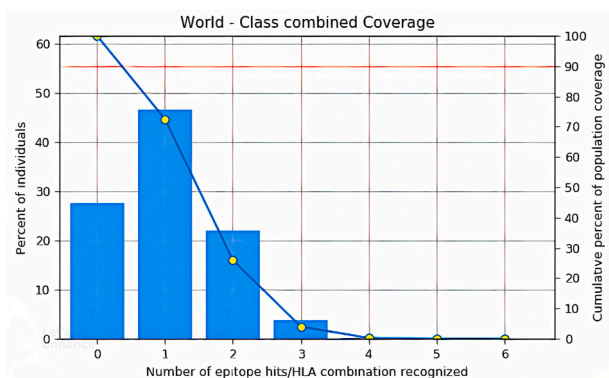


Fig. 2. Population coverage analysis of our vaccine candidate.

construct was 441AA containing one NY-ESO-1 protein subunit, one subunit from MAGE-1, two subunits from SSX protein joined by AYY linker, an adjuvant joined by EAAAK and a histidine tag joined with RVR linker (Fig. 1). All the selected subunits were probable antigenic (Table 3).

3.6. Antigenicity, allergenicity and other physicochemical properties analysis

Our vaccine candidate was 441AA, having molecular weight of about 46575.98 Da. Vaccine candidate was probable antigen having antigenicity 0.6139 and 0.752170 predicted by VaxiJen 2.0 and AntigenPro respectively. Vaccine construct was probable antigen and non-allergenic. ToxinPred was used for the prediction of toxicity and is non-toxic. Other physical and chemical parameters were evaluated by ProtParam. Solubility was calculated to be 0.973. Theoretical pI, instability index and GRAVY value was reported as 6.5, 35.39 and -0.314 .

3.7. Population coverage analysis

Vaccine candidate should cover a wide population of human. IEDB population coverage analysis tool was used to calculate the coverage of our vaccine candidate in worldwide population against 14 Class-I and class-II combined HLA alleles. Graphical results suggested that our vaccine candidate covers 72.48 % of human population worldwide (Fig. 2).

3.8. Prediction of secondary structure

PsiPred and GOR by Prabi are used for predicting secondary structure. The predicted results suggested that our vaccine construct contained 47.39 % alpha helix, 0.0 % beta turns and bent regions, 46.26 % random coils and 6.35 % extended strand. Graphical depiction of our vaccine construct's secondary structure predicted by PsiPred are exhibited (Fig. 3).

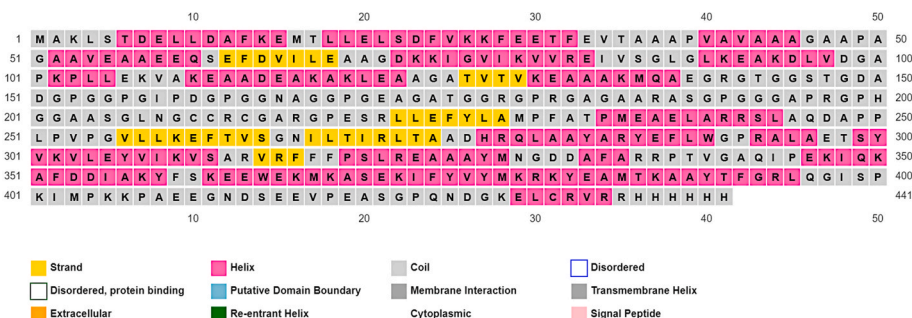


Fig. 3. Secondary structure of our vaccine candidate predicted by PsiPred.

3.9. Prediction, refinement and validation of tertiary structure

AlphaFold incorporated in ChimeraX was used for predicting tertiary structure of vaccine candidate which was further validated and refined. Predicted AlphaFold structure was refined by GalaxyRefine server. GalaxyRefine proposed 5 models with different parameters i.e., GDT-HA, RMSD, MolProbity, Clashscore, Poor rotamers and RAMA favored score (Table 4). Model 1 was selected because it had the best quality scores and had the most stability. GDT-HA (Global Distance Test-High Accuracy) calculates the deviation of predicted refined structure from the reference structure. The refined Model 1 had the lowest GDT-HA as it was least distant from the initial model. RMSD (Root Mean Square Deviation) calculates the atomic distance in the protein chain. Model 1 had the lowest RMSD value. Lowest the RMSD value, most stable the tertiary structure. MolProbity score suggests the crystallographic clarification of the structure. Our selected model had the MolProbity score of 1.372 which was less than the initial predicted model, thus representing higher resolution of refined model. Clashscore indicates the number of unfavorable clashes in the protein structure [50]. Our selected model had the lowest class score i.e., 3.9 much lower than the class score of initial structure i.e., 37.7. RAMA favored reflects the clustered secondary structures in the protein tertiary structure. Model 1 had 96.8 % RAMA favored regions, much more than of initial region. These quality scores represent overall good quality of Model 1 (Fig. 4A). Tertiary structure was then validated by evaluating Z-score, Ramachandran plot and Molprobity score. ProSA server was used for the determination of overall model quality and Z-score (Fig. 4B). Z-score of our refined model was -7.12 which is within the extend for stable proteins of the same molecular weight. Ramachandran plot was generated by Molprobity server. Ramachandran plot shows that 96.8 % residues were in the favored regions and 99.1 % of residues were in the allowed regions reflecting high stability of the structure. 4 outliers (phi, psi) were observed 100 Ala (49.3, -103.6), 146 Ser (83.8, 129.1), 198 Gly (173.6, 82.9), 251 Leu (74.2, 140.8). Molprobity score was 1.18 and class score of 2.14 (Fig. 4C).

3.10. Prediction of conformational epitopes

Conformational epitopes were predicted using the tertiary structure of vaccine by ElliPro server. Six discontinuous B-cell epitopes with a significant score of 0.7–0.8 were determined. We found 92 residues with

Table 4
Quality score of refined models predicted by GalaxyRefine.

Model	GDT-HA	RMSD	MolProbity	Clash score	Rama favored
Initial	1	0	3.487	37.7	59.2
MODEL 1	0.8628	0.733	1.372	3.9	96.8
MODEL 2	0.8617	0.736	1.434	4.3	96.6
MODEL 3	0.8571	0.744	1.407	5.1	97.3
MODEL 4	0.8634	0.723	1.531	4.3	95.4
MODEL 5	0.8594	0.749	1.49	4	95.7

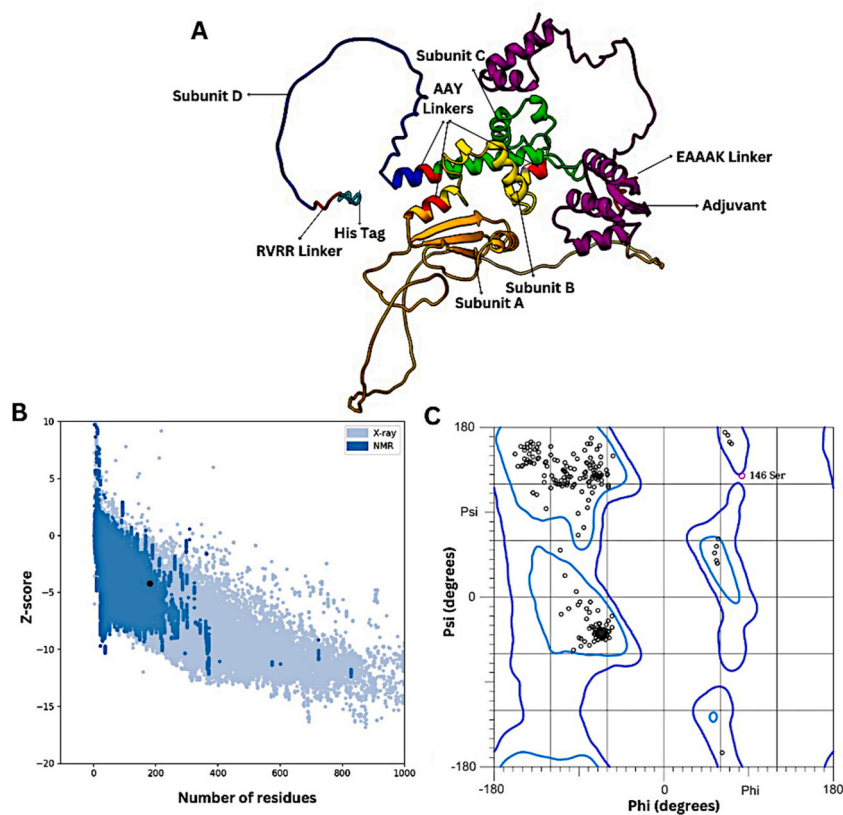


Fig. 4. (A) Tertiary structure of vaccine candidate predicted by AlphaFold and refined by GalaxyRefine; (B) Z-score refined structure predicted by ProSA server; (C) Ramachandran plot generated by Molprobiy server showing majority of the residues in favored regions.

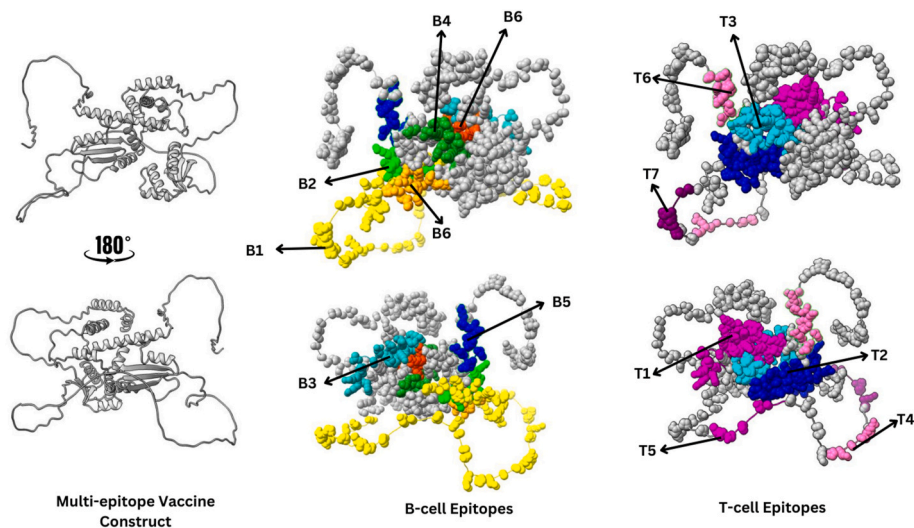


Fig. 5. 3D models of B and T cell epitopes on the surface of chimera protein.

substantial score of 0.8 and eight residues with score of 0.7. These 6 B-cell conformational epitopes and 7 T-cell conformational epitopes were mapped on the 3D structure of multi-epitope vaccine candidate (Fig. 5).

3.11. Molecular docking

Toll like receptors are mediators of inflammatory pathway that have extracellular regions that recognize parts of endogenous and exogenous antigens [51]. TLR4 has a significant role in inducing an immune response. Huma leukocyte antigen (HLA) encode antigenic

peptide-presenting surface molecules on them and thus have a role in induction and regulation of immune response. Binding of our vaccine construct with TLR4 and HLA-A*11:01 is graphically represented (Fig. 6). ClusPro generated 29 Vaccine-TLR4 and Vaccine-HLA docked models [52]. The models with the lowest binding energy were chosen. Low energy represents the stability and integrity of docked complexes. UCSF Chimera Software was used for the illustration of docked complexes. Vaccine-TLR4 complex has the -1184.8 kcal/mol lowest energy and vaccine-HLA complex had -1255.8 kcal/mol energy.

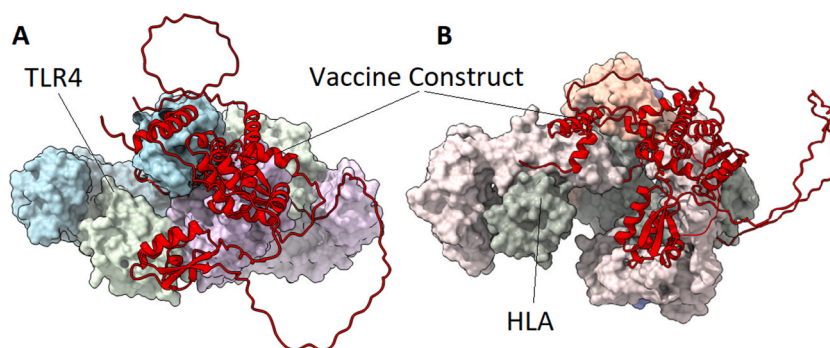


Fig. 6. (a) Docked complexes of our vaccine construct with TLR4; (b) Docked complexes of our vaccine construct with HLA-A*11:01 generated by ClusPro and visualized by ChimeraX.

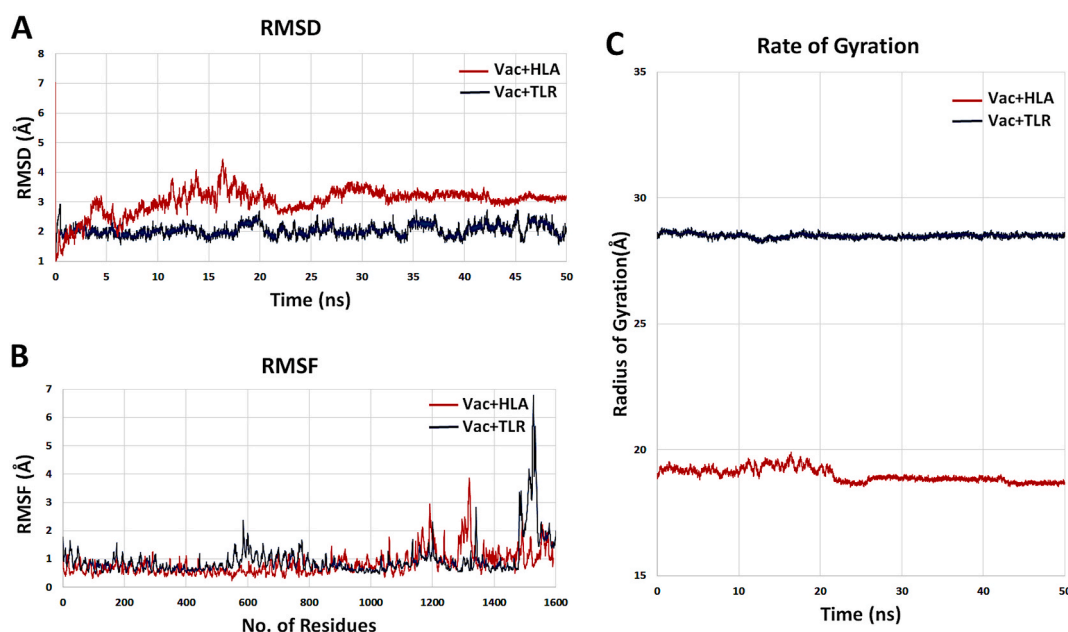


Fig. 7. The graphical representation Molecular Dynamics Simulations of Vaccine construct-TLR complex and Vaccine construct-HLA complex done through GRO-MACS software (a) Root Mean Square Deviation (RMSD) of docked complexes; (b) Root Mean Square Fluctuation (RMSF); (c) Rate of gyration of docked complexes.

3.12. Molecular dynamics simulation

Molecular dynamics (MD) simulation stands as a potent method for the analysis of biological systems, offering valuable mechanistic insights into the potential behavior of the system within a simulated biological environment. This computational technique allows for the dynamic exploration of biomolecular structures over time, providing a detailed understanding of molecular interactions, conformational changes, and the overall dynamics [53]. The production phase of molecular dynamics (MD) simulations was conducted using Gromacs 2020.4, and subsequent trajectory analysis was performed to elucidate the structural properties and interactions at a molecular level among immune receptors and the predicted vaccine protein.

Root mean square deviations (RMSD) analysis elucidate how the backbone atoms evolve in relation to their initial equilibrated positions. A lower Root Mean Square Deviation (RMSD) value indicates better stability in the corresponding system [54]. In the current study, we quantified the Root Mean Square Deviation (RMSD) in backbone atoms across the entirety of protein-protein complexes. Fig. 7A illustrates the Root Mean Square Deviation (RMSD) observed in the analyzed systems. The assessment of Root Mean Square Fluctuations (RMSF) offers valuable insights into potential variations in the secondary structure of the

investigated protein [55]. In the current study, the Root Mean Square Fluctuations (RMSF) in the side chain atoms of residues within each system were quantified. Fig. 7B depicts the Root Mean Square Fluctuations (RMSF) observed in the simulated systems. The examination of the Radius of Gyration (Rg) serves as a comprehensive measure of the overall compactness of the system [56]. Fig. 7C displays the outcomes of the total Rg analysis.

3.13. Codon optimization and cloning

For the cloning and expression of our vaccine candidate in prokaryotic systems, codon was improved for recombinant gene expression by Java Codon Optimization Tool using the FASTA sequence of vaccine. Total sequence after optimization were 1323 nucleotides. GC content of refined sequence was 73.02 and Codon Adaptation Index value was 0.96. After the optimization, Snapgene software was used for the insertional cloning. Two common restriction sites EcoR1 and Nde1 were attached at the both ends of optimized codon sequence and then inserted into pET28a (+) expression vector. The codon sequence was inserted into EcoR1 and Nde1 sites, forming a recombinant vector of 6626bp. Inserted vaccine sequence is shown in red in recombinant vector (Fig. 8A). Further, for the validation of cloning, agarose gel simulation

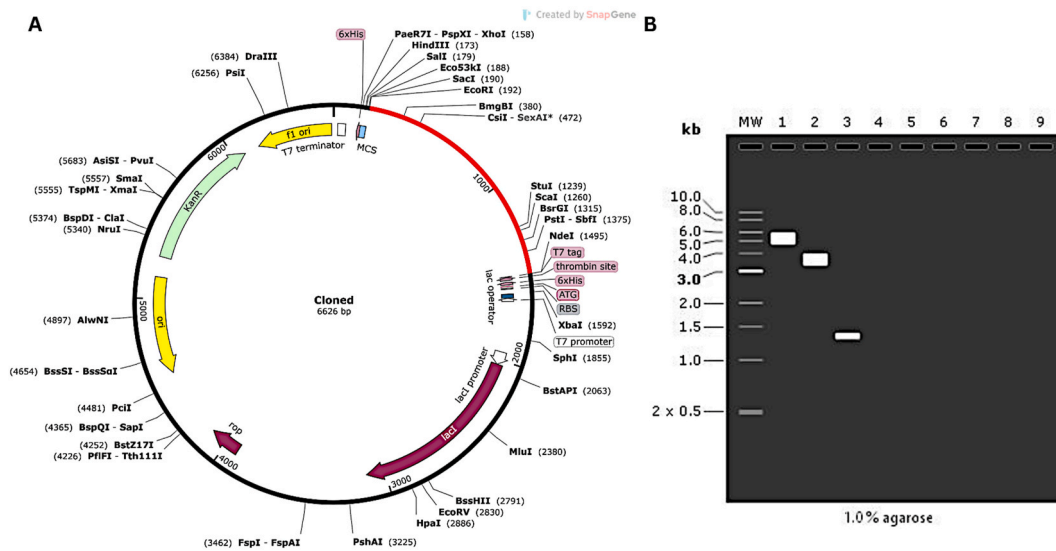


Fig. 8. (a) Schematic diagram of cloning our vaccine construct in Pet28a(+) vector; (b) Cloned pET28a (+) vector with our vaccine construct in red; (d) Gel Electrophoresis to confirm the cloning of our vaccine construct. Lane #1 showing the cloned pET28a (+) vector (6626), Lane#2 showing the pET28a (+) without the insert (5369bp) and Lane#3 showing the band of our vaccine construct (1335bp). (For interpretation of the references to colour in this figure legend, the reader is referred to the Web version of this article.)

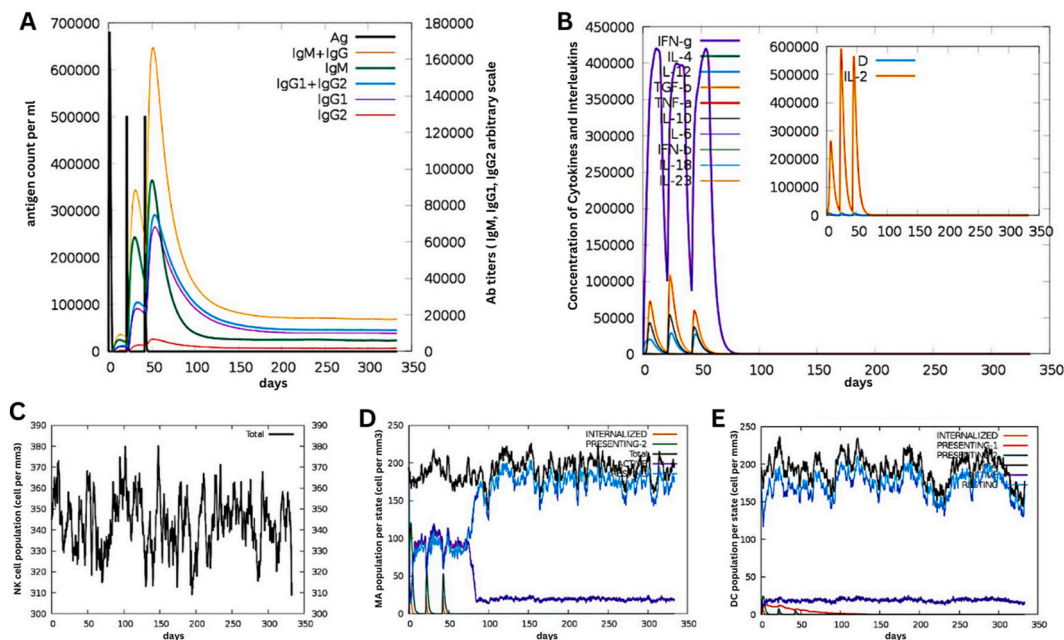


Fig. 9. (a) Concentration of antigen, immunoglobins and their complexes; (b) Concentration of cytokines and interleukins; (c) Natural killer, Macrophages and Dendritic cellular population during the course of immunization.

was performed using the Snappgene software. 1 % agarose gel simulation was done, and as a buffer solution, Tris-Borate-EDTA was selected. The outcomes show that the vector was successfully cloned with our vaccine design (Fig. 8B).

3.14. Immune simulation

Theoretical immune response of our vaccine candidate was generated by C-ImmSim server. The generated graphical results show that immune response was exponentially increased after 3rd dose followed by a drop in antigen concentration (Fig. 9). The significant level of IFN γ and IL-2 after triggering immune response was observed followed by the increased concentration of natural killer cells, macrophages and dendritic cell after inducing immune response.

4. Discussion

Cutaneous melanoma (CM), the most challenging and lethal type of skin cancer, is a multifactorial disease [57] with ongoing treatment challenges involving rapid progression to metastatic cutaneous melanoma, which results in numerous recurrences even after surgery and, most remarkably, the low response rates and resistance to the available treatments, especially when it comes to incurable metastatic CM. Therefore, different innovative therapeutic procedures for CM are needed to be implemented [58]. Reverse vaccinology, inception in 2000 as a plethora of computational processes allowing the analysis of pathogen genomics and identification of potential proteins and peptides but now, twenty-two years later, reverse vaccinology has revolutionized in computational vaccinology, drug discovery and subtractive proteomics

[59]. In this study, Melanoma-associated Cancer/Testis antigens (CTAs) were targeted for designing multi-epitope vaccine candidate. CTAs are onco-fetal proteins and their expression is restricted in male germ cells and re-expression in several malignancies [60]. Among 48 CTAs that were identified and studied in melanoma, NY-ESO-1, MAGE-1 and SSX2 were the most antigenic and expressive in primary and malignant melanoma [22].

After epitope prediction of our target antigens, four epitope rich domains were selected and fused together with linkers along with a molecular adjuvant. Selection of adjuvant and linkers is a critical step in multi-epitope vaccine development. 50S ribosomal protein L7/L12 is extracted from Mycobacterium tuberculosis and have role in the enhancement of dendritic cells, and polarization of CD4⁺ and CD8⁺ cells [61], and can effectively provoke the function vaccine candidate. AAY linker improve antigenic presentation [62], EAAAK linker improve stability of the construct [63], and RVRRL improve epitope separation [64].

Our vaccine construct was 441AA. Size was about 46 kDa which is reasonable because proteins less than 110 kb is easier for expression and purification [65]. Our vaccine construct was non-allergen and non-toxic indicating that vaccine will elicit a suitable immune response without any potential side effect. Theoretical pI was calculated as 6.5, which show that vaccine construct is acidic in nature [66]. Instability index was 35.39, and proteins that have an instability score below 40 are considered to be stable in nature. GRAVY was -0.314 and this value indicates that vaccine construct is hydrophilic [67]. After the secondary and tertiary structures are predicted, tertiary structure was validated by evaluating Z-score and Ramachandran plots. Z-score calculates the energy deviation of the structure with respect to random conformations and indicates the overall model quality [68]. Ramachandran plots indicated that 96.8 % residues were in the favored regions and 99.1 % of residues were in the allowed regions reflecting high stability of the structure [69]. Vaccine construct was docked with HLA and TLR4 and result indicates the fine interaction between the ligand and the receptors. Then Vaccine-TLR4 and Vaccine-HLA complexes were subjected to MD simulation. MD simulation through GROMACS shows that our docked complexes are stable. For insilico cloning in pET28a (+) vector, codons were optimized. GC content of refined sequence was 73.019 and Codon Adaptation Index value was 0.96. CAI value should be higher than 0.8 for the effective cloning and expression in the vector system [70]. All the results obtained were satisfactory.

Funding

This research did not receive any financial support.

CRediT authorship contribution statement

Sana Khalid: Conceptualization, Formal analysis, Methodology, Writing – original draft. **Jinlei Guo:** Formal analysis. **Syed Aun Muhammad:** Conceptualization, Formal analysis, Methodology, Supervision, Writing – review & editing. **Baogang Bai:** Formal analysis, Writing – review & editing.

Declaration of competing interest

The authors declare that they have no known competing financial interests or personal relationships that could have appeared to influence the work reported in this paper.

Data availability

Available with Manuscript

Appendix A. Supplementary data

Supplementary data to this article can be found online at <https://doi.org/10.1016/j.bbrep.2024.101651>.

References

- [1] A.J. Sober, Diagnosis and management of skin cancer, *Cancer* 51 (S12) (1983) 2448–2452.
- [2] H. Sung, J. Ferlay, R.L. Siegel, M. Laversanne, I. Soerjomataram, A. Jemal, et al., Global cancer statistics 2020: GLOBOCAN estimates of incidence and mortality worldwide for 36 cancers in 185 countries, *CA A Cancer J. Clin.* 71 (3) (2021) 209–249.
- [3] D. Cerezo-Wallis, M. S Soengas, Understanding tumor-antigen presentation in the new era of cancer immunotherapy, *Curr. Pharmaceut. Des.* 22 (41) (2016) 6234–6250.
- [4] C.M. Balch, S.-J. Soong, J.E. Gershenwald, J.F. Thompson, D.S. Reintgen, N. Cascinelli, et al., Prognostic factors analysis of 17,600 melanoma patients: validation of the American Joint Committee on Cancer melanoma staging system, *J. Clin. Oncol.* 19 (16) (2001) 3622–3634.
- [5] Y.-T. Chen, M.J. Scanlan, U. Sahin, Ö. Türeci, A.O. Gure, S. Tsang, et al., A testicular antigen aberrantly expressed in human cancers detected by autologous antibody screening, *Proc. Natl. Acad. Sci. USA* 94 (5) (1997) 1914–1918.
- [6] S. Faramarzi, S. Ghafouri-Fard, Melanoma: a prototype of cancer-testis antigen-expressing malignancies, *Immunotherapy* 9 (13) (2017) 1103–1113.
- [7] S.-J. Jang, J.-C. Soria, L. Wang, K.A. Hassan, R.C. Morice, G.L. Walsh, et al., Activation of melanoma antigen tumor antigens occurs early in lung carcinogenesis, *Cancer Res.* 61 (21) (2001) 7959–7963.
- [8] M.J. Scanlan, A.O. Gure, A.A. Jungbluth, L.J. Old, Y.T. Chen, Cancer/testis antigens: an expanding family of targets for cancer immunotherapy, *Immunol. Rev.* 188 (1) (2002) 22–32.
- [9] K.Ö. Forslund, K. Nordqvist, The melanoma antigen genes—any clues to their functions in normal tissues? *Exp. Cell Res.* 265 (2) (2001) 185–194.
- [10] Ö. Türeci, U. Sahin, I. Schobert, M. Koslowski, H. Schmitt, H.-J. Schild, et al., The SSX-2 gene, which is involved in the t (X; 18) translocation of synovial sarcomas, codes for the human tumor antigen HOM-MEL-40, *Cancer Res.* 56 (20) (1996) 4766–4772.
- [11] E. Stockert, E. Jäger, Y.-T. Chen, M.J. Scanlan, I. Gout, J. Karbach, et al., A survey of the humoral immune response of cancer patients to a panel of human tumor antigens, *J. Exp. Med.* 187 (8) (1998) 1349–1354.
- [12] E. Jäger, S. Gnjatic, Y. Nagata, E. Stockert, D. Jäger, J. Karbach, et al., Induction of primary NY-ESO-1 immunity: CD8⁺ T lymphocyte and antibody responses in peptide-vaccinated patients with NY-ESO-1+ cancers, *Proc. Natl. Acad. Sci. USA* 97 (22) (2000) 12198–12203.
- [13] S.S. Usmani, R. Kumar, S. Bhalla, V. Kumar, G.P. Raghava, In silico tools and databases for designing peptide-based vaccine and drugs, *Advances in protein chemistry and structural biology* 112 (2018) 221–263.
- [14] R. Anand, S. Biswal, R. Bhatt, B.N. Tiwary, Computational perspectives revealed prospective vaccine candidates from five structural proteins of novel SARS corona virus 2019 (SARS-CoV-2), *PeerJ* 8 (2020) e9855.
- [15] Z. Yazdani, A. Rafiei, M. Yazdani, R. Valadan, Design an efficient multi-epitope peptide vaccine candidate against SARS-CoV-2: an in silico analysis, *Infect. Drug Resist.* (2020) 3007–3022.
- [16] F. Shahid, T. Zaheer, S.T. Ashraf, M. Shehroz, F. Anwer, A. Naz, et al., Chimeric vaccine designs against *Acinetobacter baumannii* using pan genome and reverse vaccinology approaches, *Sci. Rep.* 11 (1) (2021) 13213.
- [17] S. Thomas, A. Abraham, J. Baldwin, S. Piplani, N. Petrovsky, Artificial intelligence in vaccine and drug design, *Vaccine Design: Methods and Protocols* ume 1 (2022) 131–146. *Vaccines for Human Diseases.*
- [18] K. Abraham Peele, T. Srihansa, S. Krupanidhi, V.S. Ayyagari, T. Venkateswarulu, Design of multi-epitope vaccine candidate against SARS-CoV-2: a in-silico study, *J. Biomol. Struct. Dyn.* 39 (10) (2021) 3793–3801.
- [19] A. Atapour, M. Negahdaripour, Y. Ghasemi, D. Razmjuee, A. Savardashtaki, S. M. Mousavi, et al., In silico designing a candidate vaccine against breast cancer, *Int. J. Pept. Res. Therapeut.* 26 (2020) 369–380.
- [20] G. Sethi, S. Sethi, R. Krishna, Multi-epitope based vaccine design against *Staphylococcus epidermidis*: a subtractive proteomics and immunoinformatics approach, *Microb. Pathog.* 165 (2022) 105484.
- [21] D.D. Martinelli, In silico vaccine design: a tutorial in immunoinformatics, *Healthcare Analytics* 2 (2022) 100044.
- [22] D. Tio, F.R. Kasiem, M. Willemsen, R. van Doorn, N. van der Werf, R. Hoekzema, et al., Expression of cancer/testis antigens in cutaneous melanoma: a systematic review, *Melanoma Res.* 29 (4) (2019) 349–357.
- [23] Y. He, Z. Xiang, H.L. Mobley, Vaxign: the first web-based vaccine design program for reverse vaccinology and applications for vaccine development, *J. Biomed. Biotechnol.* 2010 (2010).
- [24] S. Gupta, P. Kapoor, K. Chaudhary, A. Gautam, R. Kumar, G.P. Raghava, Peptide toxicity prediction, *Computational peptidology* (2015) 143–157.
- [25] V.K. Garg, H. Avashthi, A. Tiwari, P.A. Jain, P.W. Ramkete, A.M. Kayastha, et al., MFPPPI-multi FASTA ProtParam interface, *Bioinformatics* 12 (2) (2016) 74.
- [26] V. Jurtz, S. Paul, M. Andreatta, P. Marcatili, B. Peters, M. Nielsen, NetMHCpan-4.0: improved peptide-MHC class I interaction predictions integrating eluted ligand and peptide binding affinity data, *J. Immunol.* 199 (9) (2017) 3360–3368.

- [27] B. Reynisson, B. Alvarez, S. Paul, B. Peters, M. Nielsen, NetMHCpan-4.1 and NetMHCIIpan-4.0: improved predictions of MHC antigen presentation by concurrent motif deconvolution and integration of MS MHC eluted ligand data, *Nucleic Acids Res.* 48 (W1) (2020) W449–W454.
- [28] Q. Zhang, P. Wang, Y. Kim, P. Haste-Andersen, J. Beaver, P.E. Bourne, et al., Immune epitope database analysis resource (IEDB-AR), *Nucleic Acids Res.* 36 (suppl 2) (2008) W513–W518.
- [29] M. Li, Y. Zhu, C. Niu, X. Xie, G. Haimiti, W. Guo, et al., Design of a multi-epitope vaccine candidate against *Brucella melitensis*, *Sci. Rep.* 12 (1) (2022) 10146.
- [30] Z. Chen, Y. Zhu, T. Sha, Z. Li, Y. Li, F. Zhang, et al., Design of a new multi-epitope vaccine against *Brucella* based on T and B cell epitopes using bioinformatics methods, *Epidemiol. Infect.* (2021) 149.
- [31] J. Dey, S.R. Mahapatra, S. Patnaik, S. Lata, G.S. Kushwaha, R.K. Panda, et al., Molecular characterization and designing of a novel multi-epitope vaccine construct against *Pseudomonas aeruginosa*, *Int. J. Pept. Res. Therapeut.* 28 (2) (2022) 49.
- [32] C.N. Magnan, M. Zeller, M.A. Kayala, A. Vigil, A. Randall, P.L. Felgner, et al., High-throughput prediction of protein antigenicity using protein microarray data, *Bioinformatics* 26 (23) (2010) 2936–2943.
- [33] I. Dimitrov, D.R. Flower, I. Doytchinova, AllerTOP-a server for in silico prediction of allergens, *BMC Bioinf.* 14 (2013) 1–9. BioMed Central.
- [34] C.N. Magnan, A. Randall, P. Baldi, SOLpro: accurate sequence-based prediction of protein solubility, *Bioinformatics* 25 (17) (2009) 2200–2207.
- [35] L.J. McGuffin, K. Bryson, D.T. Jones, The PSIPRED protein structure prediction server, *Bioinformatics* 16 (4) (2000) 404–405.
- [36] M. Mirdita, K. Schütze, Y. Moriwaki, L. Heo, S. Ovchinnikov, M. Steinegger, ColabFold: making protein folding accessible to all, *Nat. Methods* 19 (6) (2022) 679–682.
- [37] M. Wiederstein, M.J. Sippl, ProSA-web: interactive web service for the recognition of errors in three-dimensional structures of proteins, *Nucleic Acids Res.* 35 (suppl 2) (2007) W407–W410.
- [38] V.B. Chen, W.B. Arendall, J.J. Headd, D.A. Keedy, R.M. Immormino, G.J. Kapral, et al., MolProbity: all-atom structure validation for macromolecular crystallography, *Acta Crystallogr. Sect. D Biol. Crystallogr.* 66 (1) (2010) 12–21.
- [39] J. Ponomarenko, H.-H. Bui, W. Li, N. Füsseder, P.E. Bourne, A. Sette, et al., ElliPro: a new structure-based tool for the prediction of antibody epitopes, *BMC Bioinf.* 9 (2008) 1–8.
- [40] H.M. Kim, B.S. Park, J.-I. Kim, S.E. Kim, J. Lee, S.C. Oh, et al., Crystal structure of the TLR4-MD-2 complex with bound endotoxin antagonist Eritoran, *Cell* 130 (5) (2007) 906–917.
- [41] D. Kozakov, D.R. Hall, B. Xia, K.A. Porter, D. Padhorny, C. Yueh, et al., The ClusPro web server for protein–protein docking, *Nat. Protoc.* 12 (2) (2017) 255–278.
- [42] W.L. DeLano, Pymol: an open-source molecular graphics tool, *CCP4 Newsl Protein Crystallogr* 40 (1) (2002) 82–92.
- [43] H. Liu, D. Song, H. Lu, R. Luo, H.F. Chen, Intrinsically disordered protein-specific force field CHARMM 36 IDPSFF, *Wiley Online Library* 92 (2018) 1722–1735.
- [44] A.M. Bayan, S.H. Mosawi, N. Fani, M.S. Behrad, A.J. Mehrpoor, M.Y. Noori, et al., Integrating molecular docking and molecular dynamics simulation studies on the affinity and interactions of piperine with β -lactamase class A enzymes, *J. Mol. Struct.* 1292 (2023) 136151.
- [45] A. Grote, K. Hiller, M. Scheer, R. Münch, B. Nörtemann, D.C. Hempel, et al., JCat: a novel tool to adapt codon usage of a target gene to its potential expression host, *Nucleic Acids Res.* 33 (suppl 2) (2005) W526–W531.
- [46] M. Shahab, C. Hayat, R. Sikandar, G. Zheng, S. Akter, In silico designing of a multi-epitope vaccine against *Burkholderia pseudomallei*: reverse vaccinology and immunoinformatics, *J. Genet. Eng. Biotechnol.* 20 (1) (2022) 100.
- [47] I.A. Doytchinova, D.R. Flower, VaxiJen: a server for prediction of protective antigens, tumour antigens and subunit vaccines, *BMC Bioinf.* 8 (1) (2007) 1–7.
- [48] M.A. Hossain, G. Liu, B. Dai, Y. Si, Q. Yang, J. Wazir, et al., Reinvigorating exhausted CD8⁺ cytotoxic T lymphocytes in the tumor microenvironment and current strategies in cancer immunotherapy, *Med. Res. Rev.* 41 (1) (2021) 156–201.
- [49] K.M. Adusei, T.B. Ngo, K. Sadtler, T lymphocytes as critical mediators in tissue regeneration, fibrosis, and the foreign body response, *Acta Biomater.* 133 (2021) 17–33.
- [50] T. Wu, Z. Guo, J. Cheng, Atomic protein structure refinement using all-atom graph representations and SE (3)-equivariant graph transformer, *Bioinformatics* 39 (5) (2023) btad298.
- [51] K. Takeda, T. Kaisho, S. Akira, Toll-like receptors, *Annu. Rev. Immunol.* 21 (1) (2003) 335–376.
- [52] S. Vajda, C. Yueh, D. Beglov, T. Bohnuud, S.E. Mottarella, B. Xia, et al., New additions to the ClusPro server motivated by CAPRI, *Proteins: Struct., Funct., Bioinf.* 85 (3) (2017) 435–444.
- [53] S.A. Hollingsworth, R.O. Dror, Molecular dynamics simulation for all, *Neuron* 99 (6) (2018) 1129–1143.
- [54] T. Fukutani, K. Miyazawa, S. Iwata, H. Satoh, G.-Rmsd, Root mean square deviation based method for three-dimensional molecular similarity determination, *Bull. Chem. Soc. Jpn.* 94 (2) (2021) 655–665.
- [55] D.-D. Li, T.-T. Wu, P. Yu, Z.-Z. Wang, W. Xiao, Y. Jiang, et al., Molecular dynamics analysis of binding sites of epidermal growth factor receptor kinase inhibitors, *ACS Omega* 5 (26) (2020) 16307–16314.
- [56] E. Yamamoto, T. Akimoto, A. Mitsutake, R. Metzler, Universal relation between instantaneous diffusivity and radius of gyration of proteins in aqueous solution, *Phys. Rev. Lett.* 126 (12) (2021) 128101.
- [57] M.F. Simoes, J.S. Sousa, A.C. Pais, Skin cancer and new treatment perspectives: a review, *Cancer Lett.* 357 (1) (2015) 8–42.
- [58] Z. Apalla, A. Lallas, E. Sotiriou, E. Lazaridou, D. Ioannides, Epidemiological trends in skin cancer, *Dermatol. Pract. Concept.* 7 (2) (2017) 1.
- [59] S.J. Goodswen, P.J. Kennedy, J.T. Ellis, A guide to current methodology and usage of reverse vaccinology towards in silico vaccine discovery, *FEMS (Fed. Eur. Microbiol. Soc.) Microbiol. Rev.* 47 (2) (2023) fuad004.
- [60] L. Dominick, D.L.C. Auci, Daniel Herendeen, Elizabeth K. Broussard, John B. Liao, Gregory E. Holt, Mary L. Disis, Chapter 23 - clinical Application of plasmid-based cancer vaccines, in: Gerson ECLaSL, Editor Gene Therapy of Cancer, third ed., 2014. USA.
- [61] S.J. Lee, S.J. Shin, M.H. Lee, M.-G. Lee, T.H. Kang, W.S. Park, et al., A potential protein adjuvant derived from *Mycobacterium tuberculosis* Rv0652 enhances dendritic cells-based tumor immunotherapy, *PLoS One* 9 (8) (2014) e104351.
- [62] B. Livingston, C. Crimi, M. Newman, Y. Higashimoto, E. Appella, J. Sidney, et al., A rational strategy to design multi-epitope immunogens based on multiple Th lymphocyte epitopes, *J. Immunol.* 168 (11) (2002) 5499–5506.
- [63] R. Arai, H. Ueda, A. Kitayama, N. Kamiya, T. Nagamune, Design of the linkers which effectively separate domains of a bifunctional fusion protein, *Protein Eng.* 14 (8) (2001) 529–532.
- [64] R. Mohanty, M. Manoswini, A.K. Dhal, N. Ganguly, In silico analysis of a novel protein in CAR T-cell therapy for the treatment of hematologic cancer through molecular modelling, docking, and dynamics approach, *Comput. Biol. Med.* 151 (2022) 106285.
- [65] D. Barh, N. Barve, K. Gupta, S. Chandra, N. Jain, S. Tiwari, et al., Exoproteome and secretome derived broad spectrum novel drug and vaccine candidates in *Vibrio cholerae* targeted by Piper betel derived compounds, *PLoS One* 8 (1) (2013) e52773.
- [66] E. Gasteiger, C. Hoogland, A. Gattiker, Se Duvaud, M.R. Wilkins, R.D. Appel, et al., Protein Identification and Analysis Tools on the ExPASy Server, Springer, 2005.
- [67] M. Ali, R.K. Pandey, N. Khatoun, A. Narula, A. Mishra, V.K. Prajapati, Exploring dengue genome to construct a multi-epitope based subunit vaccine by utilizing immunoinformatics approach to battle against dengue infection, *Sci. Rep.* 7 (1) (2017) 9232.
- [68] C. Cheadle, M.P. Vawter, W.J. Freed, K.G. Becker, Analysis of microarray data using Z score transformation, *J. Mol. Diagn.* 5 (2) (2003) 73–81.
- [69] K. Gopalakrishnan, G. Sowmiya, S. Sheik, K. Sekar, Ramachandran plot on the web (2.0), *Protein Pept. Lett.* 14 (7) (2007) 669–671.
- [70] S. Morla, A. Makhija, S. Kumar, Synonymous codon usage pattern in glycoprotein gene of rabies virus, *Gene* 584 (1) (2016) 1–6.